

A Nightside Magnetospheric Configuration  
as Obtained from Trapped Electrons at 1100 km.

FACILITY FORM 502	N66-82982	
	(ACCESSION NUMBER)	(THRU)
	32	none
	(PAGES)	(CODE)
	TMX 36401	
	(NASA CR OR TMX OR AD NUMBER)	(CATEGORY)

by

Donald J. Williams

The Johns Hopkins University  
Applied Physics Laboratory  
Silver Spring, Maryland

and

Gilbert D. Mead  
Goddard Space Flight Center  
Greenbelt, Maryland

April 1965

# ABSTRACT

Using data from the polar orbiting satellite 1963 38C, we have obtained the diurnal variation of trapped electrons of energies  $E_e \geq 280$  kev and  $\geq 1.2$  Mev, during magnetic quiet. This diurnal variation is measured as a latitude shift for constant electron intensity, and is obtained as a function of invariant magnetic latitude. All the data were obtained for dipole orientations within  $\pm 12^\circ$  from the normal to the earth-sun line and within  $8^\circ$  of the noon-midnight meridian. Assuming conservation of the adiabatic invariants as these trapped electrons drift in the magnetosphere, it has been possible to obtain a nightside magnetic field configuration which fits the observed diurnal variations. A dayside configuration was used which agrees with experimental observations. The nightside configuration so determined displays an "open" field line geometry and a current sheet in the magnetic equatorial plane. The field due to this current sheet is found to range from 20-40 $\gamma$  adjacent to the sheet, depending upon the radial extent of the sheet. A field line configuration in the noon-midnight meridian is presented. It was found that the nightside trapping boundary as defined by field line closure occurs at 1100 km at  $67^\circ$  and is in agreement with observed boundaries at 1100 km of  $\sim 67^\circ$  for both  $\geq 40$  kev and  $\geq 280$  kev electrons. The situation on the dayside is different and is discussed.

*Author*

Available from NASA Office and  
NASA Centers

## INTRODUCTION

Observations of a diurnal variation in the trapped electron population at high latitudes have been reported by O'Brien [1963]; McDiarmid and Burrows [1964 a and b]; and Frank et al [1964]. These observations were all concerned with electrons of energies  $\geq 40$  kev and showed that the observed diurnal latitudinal shifts at high latitude and low altitude were greater than could be explained by the conservation of the adiabatic invariants in a distorted magnetosphere as represented by the use of an image dipole [Malville, 1960]. Fairfield [1964] found that in order to obtain the large diurnal shifts, it was necessary to add to the dipole field a field normal to the equator but oppositely-directed on the dayside and nightside hemispheres, an assumption which is physically hard to justify.

Measurements of the diurnal shift of  $\geq 280$  kev trapped electrons [Williams and Palmer, 1965] showed that these higher energy electrons display a significantly smaller diurnal latitude shift during periods of magnetic quiet than do the  $\geq 40$  kev electrons. An initial qualitative analysis by Williams and Palmer [1965] suggested that the diurnal shift of  $\geq 280$  kev trapped electrons might possibly be explained by invariant conservation in a distorted magnetosphere such as described by Mead [1964]

The present more detailed quantitative study, in which the latitudinal dependence of the diurnal shift of  $\geq 280$  kev electrons is obtained, shows that the addition of a current sheet in the tail of Mead's model, leading to an "open" field line configuration in the nightside hemisphere,

is needed to fit the observed latitude shifts. By an "open" configuration we simply mean one in which northern and southern high-latitude field lines do not connect, i.e., conjugate-point phenomena are not observed. This night-side magnetic field configuration, as obtained by fitting the  $\geq 280$  kev trapped electron diurnal variations, is quite similar to the configurations recently suggested by Dessler and Juday [1965] and Axford et al [1965], and recently measured by the magnetometer on IMP-1 [Ness, 1965].

We thus find that the observed diurnal variations of high energy ( $E_e \geq 280$  kev) trapped electrons are consistent with the drift of these particles in a distorted magnetosphere under the conservation of the adiabatic invariants,  $\mu$  and  $J$ , and the conservation of energy,  $E$ .

The experimental observations, the magnetospheric distortions, and the experimental and theoretical comparisons are described in subsequent sections.

## EXPERIMENTAL RESULTS

Satellite and Experiment. A more detailed description of the satellite and the detector may be found in Williams and Smith [1965].

Briefly, the data were obtained from the satellite 1963 38C, launched on September 28, 1963 into a nearly circular polar orbit having a 1140 km apogee, 1067 km perigee,  $89.9^\circ$  inclination, and a 107.5 min. period. The satellite was magnetically aligned and displayed an oscillation of  $< \sim 6^\circ$  about the local line of force some three days after launch. Just after launch the satellite orbital plane made an angle of  $\sim 6^\circ$  with the noon-midnight meridian and was moving toward the noon-midnight meridian at the approximate rate of  $1^\circ$  per day due to the earth's motion about the sun.

The detectors of interest comprise an integral electron spectrometer sensitive to electrons in the following energy ranges:  $E_e \geq 280$  kev,  $\geq 1.2$  Mev,  $\geq 2.4$  Mev, and  $\geq 3.6$  Mev. The spectrometer detecting channels of interest have full viewing angles of  $12^\circ$  and are oriented to look out normal to the satellite alignment axis. This is well removed from the loss cone at 1100 km and the spectrometer therefore observes trapped electrons mirroring at the point of observation.

The spectrometer is essentially insensitive to protons of energy  $\leq 180$  Mev. The monitoring of an onboard proton spectrometer has shown that proton contamination is negligible for the data presented here.

Pertinent Information. In trying to arrive at an ambient configuration for the magnetospheric cavity which is consistent with the

experimental observations, we have used only data from magnetically quiet periods and have not considered any details of the observed correlation of increases in radiation cavity distortions with increases in magnetospheric distortions, as obtained during magnetically active periods [Williams and Palmer, 1965].

The data are obtained during the period October 2 through October 12, 1963, which is the magnetically quiet period used by Williams and Palmer [1965], as their period 1. During this period the satellite orbital plane was within  $8^\circ$  of the noon-midnight meridian. Some 47 day-side passes and 28 nightside passes, obtained from the NASA receiving stations at College, Alaska and Winkfield, England, have been analyzed. Little, if any, nightside data is available from the remaining stations in our station network.

The data are analyzed in terms of the invariant latitude,  $\Lambda$ , defined at satellite altitude as

$$\cos \Lambda = \sqrt{\frac{1.17}{L}}$$

where  $L$  is as defined by McIlwain [1961] and is obtained from a 48 coefficient expansions of the earth's magnetic field. Therefore, although still useful as a measure of magnetic latitude in low altitude orbits,  $L$ , as here calculated, loses its significance at altitudes of  $\geq 4$  earth radii, where distortions due to the incident solar wind are generally considered to become noticeable. When a more accurate representation of the earth's magnetic field is used in obtaining the parameter  $L$ , it becomes apparent that  $L$  is no longer constant along a real line of force which reaches out

to  $\geq 4$  earth radii, and thus offers no conceptual advantage over the second invariant,  $J = \oint p_{\parallel} ds$ , in these more distant regions.

To avoid confusion, we note here that the values of  $\Lambda$  quoted in Williams and Palmer [1965] were obtained from the surface values,  $\cos \Lambda = \frac{1}{\sqrt{L}}$ . Those values should be corrected to satellite altitude as there is a small but noticeable effect ( $\sim 1.5^\circ$ ) in the quoted latitude at which a given latitude shift is observed.

The particles being studied are trapped electrons of energies  $E_e \geq 280$  kev and  $E_e \geq 1.2$  Mev, possessing very small equatorial pitch angles. Absolute flux values, accurate to  $\sim 50\%$  in the 280 kev and 1.2 Mev channels may be obtained by multiplying the observed count rates respectively by  $5(10)^2$  (cm<sup>2</sup> sec ster)<sup>-1</sup> and  $10^3$  (cm<sup>2</sup> sec ster)<sup>-1</sup>.

Any dependence of electron intensities on B value is dwarfed by the observed diurnal shift. The B dependence might be expected to be relatively small since at low altitude and high B values, a given fractional change in the mirror point B value being observed, produces but a very small change in the equatorial pitch angle being sampled [Williams and Kohl, 1965].

Data and Data Analysis. All the data in the interval October 2 through October 12, 1963, were plotted on a scatter plot of count rate vs. latitude for both the dayside and nightside hemispheres. Composite curves, representative of the average count rates in this time interval, were then constructed from these scatter plots. This process is described and examples are shown in Williams and Palmer [1965].

We show in Figure 1, the day and night composite curves for this time interval as obtained by Williams and Palmer [1965] but now displayed as a function of latitude. We now include the composite curves for electrons of energy  $E_e \geq 1.2$  Mev and see that the higher energy electrons behave in a similar manner as the 280 kev electrons.

Looking at Figure 1 we see that the separation of the day and night curves can be explained either by (a) a vertical shift, i.e., an intensity change in the trapped electron population, which is dependent on latitude or (b) a horizontal (latitude) shift which is also dependent on latitude, or both. It turns out that (a) requires the establishment of permanent injection mechanisms and/or permanent acceleration mechanisms capable of moving the mirror points of these trapped electrons great distances up and down lines of force. Correspondingly, (b) can be accomplished by a shift in latitude of the trapped electron population being observed and might be explained simply by the azimuthal drift of the electrons in a distorted magnetosphere under the conservation of the adiabatic invariants. It is this possible explanation of the observed diurnal shift that we are investigating in this report.

Extending the results of Maeda [1964], we find that acceleration effects due to electric fields associated with daily geomagnetic variations yield energy changes of  $< 1\%$  at 280 kev. Thus, while important at low energies ( $\sim 1$  kev), these electric fields are apparently unimportant in determining trapped electron behavior at high energies ( $\geq 280$  kev). Furthermore, Maeda shows that such electric fields accelerate electrons so that peak energies are reached at local midnight. This is opposite to



the diurnal variation observed by integral threshold detectors where trapped electron intensities are higher at noon than at midnight.

The curves shown in Figure 1 are a good representation of the diurnal shift phenomenon at low altitudes and high latitudes. While useful results can be obtained from these curves, we feel that more accurate results can be obtained by using (1) data from "matched" passes only and (2) data obtained from daily averages of dayside and nightside count rate vs.  $\lambda$  plots. The main reason for this is that the curves of Figure 1 are affected by (a) slight changes in magnetic activity occurring throughout the time period and (b) an uneven distribution of the relative proportion of day and night passes throughout the time interval. This uneven distribution when coupled with the observed steady decay in intensity observed throughout the period under study [Williams and Smith, 1965; Williams and Palmer, 1965] could yield errors in the diurnal shifts as obtained from the composite curves of Figure 1. We find that such errors are indeed small but are noticeable when comparisons are made with predictions of various magnetospheric models. We shall now discuss the data analyses, (1) and (2), mentioned above.

1. Matched pass data. It is this data that yields the most accurate results for the values of the diurnal shifts at various latitudes. These matched passes are satellite passes observed by College, Alaska and Winkfield, England which, when used in conjunction with one another, trace the satellite from nightside, through the polar region and on into the dayside hemisphere, or vice versa. Such pairs of passes, being but minutes apart and on reciprocal longitudes, eliminate a great amount of the scatter

due to magnetic activity. These matched passes are as close as we are able to come to the ideal case of simultaneous observation of the day and night-side latitude profile.

Of the 13 sets of matched passes obtained, College, Alaska recorded 10 nightside and 3 dayside passes while Winkfield, England conversely recorded 3 nightside and 10 dayside passes.

Now assuming that the shifts shown in Figure 1 are due to a shift in latitude of the electron population as it drifts from the dayside to the nightside hemisphere, we have obtained from each of the matched pass pairs, the latitudes where the same count rates were observed on both the noon and midnight meridian. This was done for both the  $\geq 280$  kev and  $\geq 1.2$  Mev channels, and the results of all the matched pass sets are shown in Figure 2, where we have plotted the nighttime latitude,  $\Lambda_N$ , vs. the daytime latitude,  $\Lambda_D$ , observed for the condition of constant count rate.

Note that while there is a certain amount of scatter in the points of Figure 2, there does exist a well defined latitude dependence of the diurnal variation for high energy electrons. Also note that the  $\geq 1.2$  Mev electrons behave in the same manner as the  $\geq 280$  kev electrons. This allows the observation that high energy electrons in general behave in the same, rather well defined manner in the outer zone during periods of magnetic quiet.

There is a certain amount of "jumpiness" in the high energy electron behavior, to be sure. However, in the mean this behavior seems well regulated. This is further illustrated in Table 1, where we show the

TABLE 1

Electron Intensities ( $E_e \geq 280$  kev) at  $\lambda = 65.8^\circ$  on Noon-Midnight Meridian  
Throughout October 3, 1963

NOON			MIDNIGHT		
Time (UT)	Geographic Longitude (degrees East)	Observed Count Rate (counts/sec)	Time (UT)	Geographic Longitude (degrees East)	Observed Count Rate (counts/sec)
0020	174	64	0000	358	3
0205	147	55	1048	196	~ 1
0922	39	43	1238	169	~ 1
1106	12	41	2133	34	4
1255	345	38	2316	8	2
1449	318	87			
1632	291	62			
2336	184	49			

observed electron intensity at the noon and at the midnight meridian at various times in the day. The representative latitude shown indicates a relatively stable intensity at both the noon and midnight meridians throughout the day.

Using the mean values of all the data in Figure 2 we have obtained the amount of latitudinal shift,  $\Delta\Lambda = \Lambda_D - \Lambda_N$ , for both  $E_e \geq 280$  kev and  $E_e \geq 1.2$  Mev, and show this shift,  $\Delta\Lambda$ , as a function of daytime latitude in Figure 3. The data in Figure 3 will be compared, in a later section, with the predictions of various magnetic field models. We point out here, once again, the regularity of the mean values of the matched pass points, indicating a well defined behavior for the electron population during magnetic quiet.

The two representative bars shown in Figure 3 indicate the entire range of values seen with the data throughout the time period under study.

2. Daily averages. For each 24 hour interval in this time period, we constructed the average latitude profile for both  $E_e \geq 280$  kev and  $E_e \geq 1.2$  Mev for the noon and midnight hemispheres. Using such daily average curves to obtain, on any given day, the daytime and nighttime latitudes,  $\Lambda_D$  and  $\Lambda_N$  respectively, corresponding to a constant count rate, yields results that are less affected by uneven pass distributions and decay effects than the curves of Figure 1.

This was done for the 11 days of the time interval under study and the resulting  $\Lambda_D$  and  $\Lambda_N$  values were displayed on a plot similar to that shown in Figure 2 for the matched pass data. The resulting plot was

very similar to Figure 2 and we show in Figure 3 the mean values of all the data obtained via the method of daily averages.

We note that the daily average data shows a bit more scatter than the matched pass data. This might be expected since the daily average data will be affected by magnetic variations taking place within a 24 hour period, whereas the matched pass data is only affected by magnetic variations taking place within  $\sim 30$  min. Nevertheless, the daily average data does provide an additional check on the accuracy of the matched pass data and is seen to be consistent with the detailed trend of the dependence of the diurnal shift with latitude.

The data in Figure 3 further indicate that electrons of both  $E_e \geq 280$  kev and  $E_e \geq 1.2$  Mev behave in a similar manner, supporting the previous observation that high energy electrons in general display the same spatial behavior in the outer zone during periods of magnetic quiet.

## THEORETICAL CONSIDERATIONS

In this section we present calculations of the diurnal shift in latitude of mirroring particles which one should expect, assuming the conservation of the first two invariants and the particle energy. The first or magnetic moment invariant is given by

$$\mu = \frac{p_{\perp}^2}{2mB} = \frac{p^2}{2mB_m} \quad (1)$$

in its relativistic form [Northrop, 1963]. If energy is conserved, a consequence of the first invariant is that a particle will always mirror at the same value of magnetic field  $B_m$ . The only way that the mirror point can be raised or lowered is for the particle to be scattered or for its energy to change, due to the presence, for example, of electric fields or time-varying magnetic fields.

The second or longitudinal invariant is given by

$$J = \int_M^{M^*} p_{\parallel} ds \quad (2)$$

where the line integral is taken along the magnetic line of force between the mirror point  $M$  and its conjugate  $M^*$ . Using  $p^2 = p_{\perp}^2 + p_{\parallel}^2$  and (1), this can be rewritten as

$$J = p \int_M^{M^*} \left(1 - \frac{B}{B_m}\right)^{1/2} ds \quad (3)$$

assuming that  $p$  is constant over a bounce period. It is convenient then to define an integral invariant  $I$  having the dimensions of a length

$$I \equiv \frac{J}{p} = \int_M^{M^*} \left(1 - \frac{B}{B_m}\right)^{1/2} ds \quad (4)$$

which will be conserved so long as the momentum, and thus the energy, is conserved. This integral is independent of the particle energy and depends only on the mirror point and the magnetic field configuration. If particles do not change energy as they drift around the earth, their mirror points will always be found on a line of constant  $I$ , assuming, of course, that they are not scattered. If loss rates and production rates are slow compared with one drift period (about 1/2 hour for 280 kev electrons at  $L = 5$ ), one would therefore expect to find approximately equal fluxes of mirroring particles at every point of constant  $B_m$  and  $I$ . The shortest decay times for trapped electrons at these latitudes has been observed to be 1/2 to 1 day, which is more than 10 times as long as the drift times [Williams and Smith, 1965].

Under the above set of assumptions, therefore, the problem of predicting the diurnal shift in latitude of mirroring particles reduces to that of calculating the integral invariant  $I$  at constant  $B_m$  as a function of latitude, longitude, and local time, and determining the locus of points where  $I$  is constant. In the present instance, we may eliminate the effect of local field irregularities due to non-dipolar terms, since the counting rates have been expressed as a function of invariant latitude in an equivalent dipole field. Thus, latitude and local time are the important variables.

In order to calculate  $I$ , one must have a model of the magnetic field. Three such models are used here. The first is that given by Mead [1964] and is based on the solution to the Chapman-Ferraro problem of a solar wind perpendicularly incident on a dipole field. A surface is formed which separates the earth's field from the infinitely-conducting, field-free solar wind. The currents on this surface, or magnetopause, modify the field inside the magnetosphere, the major effect being a general compression of the field lines. The resulting distortion of the magnetic field can most conveniently be described in terms of a spherical harmonic expansion, the coefficients determined by making a least-squares fit to the distorted field as calculated at a number of points inside the magnetosphere. This distortion depends on the strength of the solar wind, and in Mead's model this dependence is brought in through the parameter  $r_b$ , the distance to the boundary in the solar direction.

The shape of the field lines in the noon-midnight meridian plane is shown in Figure 4 of Mead [1964] for the case  $r_b = 10$  earth radii. It is seen there that the effect of field-line compression is negligible for lines emerging from latitudes less than  $60^\circ$  ( $L = 4$ ). At higher latitudes the effect becomes significant, and at  $\lambda = 75^\circ$ , where the dipole line would normally cross the equator at about  $15 R_e$ , the equatorial crossing distances in the distorted field are  $8.7$  and  $11.2 R_e$  on the noon and midnight meridians, respectively. Thus, the surface currents compress the field lines on both the day side and the nightside, although not as much on the nightside.



The integral invariant as defined by (4) was calculated as a function of latitude on the noon and midnight meridians for particles mirroring at 1100 km (geocentric distance of 1.17 earth radii). The results for the dipole field plus surface current field (hereafter referred to as  $B_d + B_s$ ) for  $r_b = 10 R_e$  are shown in Figure 4. The day-night change in latitude for constant  $I$  is seen to be about 1 degree at  $70^\circ$ . Somewhat similar results were obtained by Malville [1960], who made similar calculations using an image dipole model.

Thus, a simple compression of the magnetosphere by means of surface currents does not predict the observed shifts of several degrees at  $70^\circ$ . However, recent magnetic field measurements by Ness [1965] in the tail of the magnetosphere by the IMP-1 satellite has shown that the field configuration in this region is much different from that given by Mead's model. Beyond 10 earth radii, the field in the tail is found to be predominantly in the solar or anti-solar direction, instead of perpendicular to the magnetic equator. In addition, a neutral surface separating anti-solar directed fields in the southern hemisphere from solar directed fields in the northern hemisphere has been detected over a large extent in area. The presence of such a neutral sheet implies that plasma currents inside the magnetosphere contribute strongly to the magnetic field configuration in the tail region. The presence of such internal plasmas are specifically excluded from the usual Chapman-Ferraro problem, however. This suggests that Mead's model should be modified to take into consideration the presence of these plasma currents.

The simplest way to do this is to vectorially add an additional tail field,  $B_T$ , which is directed away from the sun in the southern hemisphere and towards the sun in the northern hemisphere. Such a field would be produced by an infinite sheet of current in the equatorial plane directed opposite to the earth's orbital velocity vector. The integral invariant on the midnight meridian for a  $60\gamma$  tail field (denoted by  $B_d + B_s + B_T (60\gamma)$ ) has been calculated and is shown in Figure 4.

If the plasma currents producing the additional field in the tail are strongest in the region past 8 or 10 earth radii, the resulting field due to these currents will not be simply directed away from or towards the sun, but will also have a southward component opposing the earth's dipole field, as pointed out by Axford et al [1965]. Such a configuration can be roughly approximated by that of a truncated semi-infinite current sheet which does not begin until some distance in back of the earth. The geometry is shown in Figure 5. The field due to such a current sheet is given by

$$B_x = -2j(\theta_2 - \theta_1)$$

$$B_y = 2j \log \frac{r_2}{r_1}$$

where  $j$  is the current per unit length in the sheet. The current sheet must have both an inner and an outer cutoff in order to avoid a logarithmic infinity in the value of  $B_y$ .

The magnetic field configuration in the noon-midnight meridian plane due to the addition of such a current sheet (the total field denoted by  $B_d + B_s + B_{CS} (40\gamma)$ ) has been calculated and is shown in Figure 6. The

current sheet begins at  $10 R_e$  in back of the earth and cuts off arbitrarily at  $40 R_e$ . The current strength is such as to produce a field of  $40\gamma$  immediately adjacent to the sheet. This configuration may be compared to Figure 4 of Mead [1964]. The major difference lies in the direction and strength of the field in the tail region. In the earlier model the field lines were roughly perpendicular to the solar direction in the equatorial region. This is still true in the present model out to about 7 earth radii, but past this point the field lines are open and lie parallel to the current sheet. The latitude separating the closed lines from the open lines on the night side is  $69^\circ$  at the earth's surface, or  $67^\circ$  at an altitude of 1100 km. Thus, one would not expect to find particles trapped above  $\sim 67^\circ$  on the nightside at 1100 km, and the second invariant is no longer defined above this latitude.

The integral invariant corresponding to this field configuration on the nightside was calculated and is shown in Figure 4. One sees that the effect of a finite current sheet producing a  $40\gamma$  field is greater than that of an infinite sheet producing a  $60\gamma$  field. The reason is due to the presence of the southward component with the finite current sheet. This component, together with the parallel component, is more effective in extending field lines than the parallel component alone. For high-latitude, low-altitude mirroring particles, the integral invariant is essentially a measure of the length of the field line, since the integral is essentially unity except immediately adjacent to the mirror points. Thus, any phenomena which tend to stretch out the field lines on the nightside will enhance the day-night latitude shift. Conversely, anything which tends

to compress the lines further on the dayside, such as an increase in solar wind intensity, will also enhance the day-night difference. A closer boundary plus a reduced current sheet field would produce about the same results. The configuration on the dayside, however, was chosen to match the observed boundary position of about  $10 R_e$  in the solar direction during quiet periods.

## DISCUSSION

We present in Figure 7 a comparison of the experimental observations of the latitude shift,  $\Delta\lambda$ , with the computed shift for various magnetospheric configurations, based on particle drift motions through the magnetosphere under the conservation of the adiabatic invariants. The theoretical curves shown in Figure 7 are obtained directly from the  $I$  vs.  $\lambda$  curves presented in Figure 4.

Because both electron energies studied,  $E_e \geq 280$  kev and  $\geq 1.2$  Mev, display the same diurnal variation, we show only the  $E_e \geq 280$  kev data in Figure 7 and consider it to be representative of high energy trapped electrons in general. The bars shown indicate the entire range of values seen in this time period.

It is seen from Figure 7 that of the field configurations studied, the one employing the original model of Mead [1964] plus a current sheet located in the magnetospheric tail,  $B_d + B_s + B_{CS}$  (40 $\gamma$ ), best fits the experimental observations.

A truncated semi-infinite current sheet will obviously lead to inconsistencies when the field configuration away from the noon-midnight meridian is considered. However, the data are all obtained within  $8^\circ$  of the noon-midnight meridian and such a current sheet should yield results which may appropriately be compared with the data.

The form of the current sheet, extending radially from  $10 R_e$  to  $40 R_e$  and being of constant magnitude, is to some degree, arbitrary. A

more appropriate current distribution, one which decreases in magnitude at large radial distances [Ness, 1965] might be preferable. In general, moving the front edge of the current sheet in closer to the earth's surface or extending the sheet further away from the earth and simultaneously lowering the current will give a satisfactory fit to the data. In Table II we show two additional current sheet configurations which also fit the observed trapped electron diurnal variations.

We note that while the field strengths near the current sheet agree with some of the measurements reported by Ness [1965] in the tail region, they are in general somewhat higher than his observations. For example, Ness shows that the field in the tail region decreases to  $\sim 10\gamma$  at  $30 R_E$ , whereas all our values are somewhat larger than this (the field due to the dipole plus surface currents is negligible in this region). There are perhaps two basic physically significant reasons for this disagreement. (1) The effects of a ring current have been neglected and will have to be included when more is known about the characteristics of such a source. Outside the ring current, the field is decreased and a relatively larger field line extension will take place on the nightside hemisphere, thereby reducing the current sheet intensity below our values required to match the diurnal shifts. (2) A more realistic current distribution should match the nightside radial B variation [Ness, 1965]. Such a distribution probably extends significantly further out than 40 earth radii and would thus produce roughly the same effect as the current distribution used above.

TABLE II

Current Sheet Parameters Yielding Fits to the  
Experimental Observations

Front Edge of Current Sheet (earth radii)	Rear Edge of Current Sheet (earth radii)	Field Strength Adjacent to Sheet (gammas)
10	40	40
8	40	33
8	100	23

Nevertheless, the results of this analysis indicate the nightside geomagnetic field is an "open" tail configuration and that the current sheet parameters required to fit the trapped electron data are compatible with the few direct observations available in the nightside magnetic field.

Noon and midnight high latitude cutoffs for trapped 40 kev electrons have been reported by O'Brien [1963], McDiarmid and Burrows [1964a], and Frank et al [1964]. These measurements all show the following general characteristics for the high latitude boundary of trapping for  $\geq 40$  kev electrons; the average noontime high latitude cutoff at  $\sim 1100$  km is in the range  $74^\circ \lesssim \Lambda_D \lesssim 76^\circ$  whereas the average midnight boundary at  $\sim 1100$  km is in the range  $67^\circ \lesssim \Lambda_N \lesssim 69^\circ$ . Further, using the iso-intensity contours given in Frank et al [1964], we have constructed a  $\Delta\Lambda$  vs.  $\Lambda_D$  plot for  $\geq 40$  kev electrons in the noon-midnight meridian and show the results in Figure 8 where we also show for comparison the  $\geq 280$  kev results. Note that  $\Lambda_D$  is given for an altitude of 1100 km. Figure 8 clearly shows that  $\geq 40$  kev trapped electrons undergo significantly larger diurnal shifts than do  $\geq 280$  kev electrons.

The results of Williams and Palmer [1965] show that at an altitude of 1100 km during times of relative magnetic quiet, the average noontime and midnight high latitude trapping boundaries for  $\geq 280$  kev electrons are  $\sim 68.5^\circ$  and  $\sim 66^\circ$  respectively. Further, the maximum quiet time noon and



midnight trapping boundaries observed were  $70^\circ$  and  $67^\circ$  respectively. These observations indicate that both  $\geq 40$  keV and  $\geq 280$  keV electrons possess a nightside high latitude trapping boundary of  $\sim 67^\circ$  at 1100 km. This is in good agreement with the field configuration shown in Figure 5 which yields a nightside latitude boundary of  $67^\circ$  at 1100 km. This latitude corresponds to the lowest latitude field line which displays an "open" characteristic, i.e., is not connected at the equator.

Thus, the differences in the  $\geq 40$  keV and  $\geq 280$  keV trapped electron spatial characteristics, as shown in Figure 8, seem to be associated with the sunlit hemisphere. It is here that  $\geq 40$  keV trapped electrons are found at significantly higher latitudes than  $\geq 280$  keV trapped electrons, in contrast to the nightside situation where the high latitude boundary is the same for both  $\geq 40$  keV and  $\geq 280$  keV electrons. All this is consistent with the existence of a permanent injection (or acceleration) mechanism on the sunlit portion of the magnetosphere. This hypothesis [O'Brien, 1963] is further strengthened by observations of a dayside maximum in the  $\geq 40$  keV precipitated electron intensities [McDiarmid and Burrows, 1964b; Frank et al, 1964]. The relative behavior of the  $\geq 40$  keV and  $\geq 280$  keV electrons imposes a reasonable energy dependence on the injection processes.

The comparison of the  $\geq 40$  keV and  $\geq 280$  keV electron trapping boundary is subject to uncertainties due to the large temporal variations observed in these intensities. However, the results of Williams and Palmer, [1965] show that the  $\geq 40$  keV data would all have had to been obtained from periods of intense magnetic activity to explain the larger shifts observed

for the  $\geq 40$  kev electrons. The  $\geq 40$  kev observations have in fact been taken during periods of low to moderate activity [O'Brien, 1963; McDiarmid and Burrows, 1964a and b; Frank et al, 1964]. Thus, the differences do not seem to be due to differences in magnetic activity.

Another source of uncertainty in the relative  $\geq 40$  kev and  $\geq 280$  kev electron trapping boundary is the effect of a varying dipole orientation in the solar wind. The  $\geq 280$  kev trapped electron data come from within  $\sim 8^\circ$  of the noon-midnight meridian in October, a time when the dipole axis varies  $\sim \pm 12^\circ$  from the normal to the earth-sun line. The  $\geq 40$  kev data are obtained presumably from all orientations observed and are not knowingly restricted to any preferred orientation. The agreement among the observations at  $\geq 40$  kev implies that either the dipole orientation produces only a small effect at most or that long-enough time intervals were sampled so that reproducible averages over dipole orientation were obtained. In either case, comparisons with the  $\geq 280$  kev data should be significant.

## SUMMARY AND CONCLUSIONS

The spatial distribution of high energy ( $E_e \geq 280$  kev) trapped electrons in the outer zone during periods of magnetic quiet is consistent with the drift of these particles through a distorted magnetosphere, under the conservation of the adiabatic invariants. The similarity in the behavior of  $\geq 280$  kev and  $\geq 1.2$  Mev trapped electrons allows the above conclusion to extend to high energy electrons in general.

Detailed observations of the diurnal shift of high energy trapped electrons ( $E_e \geq 280$  kev and  $\geq 1.2$  Mev) in the noon-midnight meridian were obtained as a function of invariant latitude during magnetic quiet at a time when the earth's magnetic dipole axis varied  $\sim \pm 12^\circ$  from the normal to the earth-sun line. Then, using a dayside magnetic field configuration chosen to agree with the measurements of Ness et al [1964], a nightside magnetic field configuration was determined by a best fit to the measurements of the trapped electron diurnal variations. The resulting magnetic field is shown in Figure 6 and is seen to have "open" configuration due to a current sheet located in the magnetic equatorial plane. This current sheet is a truncated semi-infinite sheet extending radially from  $10 R_e$  to  $40 R_e$  and gives a field strength of  $40\gamma$  adjacent to the sheet surface. Field lines due to the sheet alone are also shown in Figure 6. Variations of the current sheet parameters are possible and are discussed in the text. This nightside field configuration, as determined by trapped electron behavior at high latitude and low altitude, is quite consistent with the direct measurements which do exist at  $\geq 10 R_e$  in the nightside hemisphere

[Ness, 1965] and agrees closely with the configurations recently suggested by Dessler and Juday [1965] and Axford, Petschek and Siscoe [1965].

Therefore, we conclude that the observations of the diurnal variation of high energy ( $E_e \geq 280$  kev) trapped electrons is consistent with the motion of these electrons in such a distorted magnetosphere under conservation of  $\mu$ ,  $J$  and  $E$ .

Using this configuration, we can make the further observation that the average behavior of high energy electrons ( $E_e \geq 280$  kev) during magnetic quiet is well ordered and stable, apart from a steady decay of particles from these low altitude regions. The observed decay times are in general much longer than the particle drift periods in these regions [Williams and Palmer, 1965] and thus also imply a certain amount of stability to the trapped population.

Finally, we note that at 1100 km both the  $\geq 40$  kev and  $\geq 280$  kev trapped electrons exhibit the same high latitude boundary of  $\sim 67^\circ$  at midnight. This agrees well with the high latitude boundary of closed field lines of  $67^\circ$  in the nightside magnetic field configuration obtained in this study. However, the dayside trapping boundary for  $\geq 40$  kev electrons extends to significantly higher latitudes than the boundary for  $\geq 280$  kev electrons. This yields the larger diurnal shifts obtained for the  $\geq 40$  kev electrons [O'Brien, 1963; McDiarmid and Burrows, 1964a and b; and Frank et al, 1964] and implies a source mechanism operating on the sunlit hemisphere.

## ACKNOWLEDGMENT

This research was supported in part by the Bureau of Naval Weapons, Department of the Navy, under Contract N0w 62-0604-c and in part by a National Aeronautics and Space Administration Grant.

## FIGURE CAPTIONS

1. Day and night count rate vs.  $\Lambda$  composite curves for the magnetically quiet period October 2-12, 1963. Curves are shown for both  $E_e \geq 280$  kev and  $\geq 1.2$  Mev. No night data are available for  $\Lambda \lesssim 55^\circ$ .  $\Lambda$  is defined at satellite altitude:  $\cos \Lambda = \frac{1.17}{L}$ .
2. Plot of  $\Lambda_N$  vs.  $\Lambda_D$  for condition of constant count rate. All matched pass data are shown, both for  $E_e \geq 280$  kev and  $E_e \geq 1.2$  Mev. For the case of no solar wind (a pure dipole field), the data would lie on the  $\Lambda_N = \Lambda_D$  line.
3. Plot of the latitude shift,  $\Delta\Lambda = \Lambda_D - \Lambda_N$ , vs. noontime latitude,  $\Lambda_D$ . Matched pass data points are obtained from the mean values of the data shown in Figure 2. Daily average data points are also mean values obtained from data similar to that shown in Figure 2. See text for discussion. Bars represent entire spread of values observed during the time period October 2-12, 1963.
4. Plot of the integral invariant,  $I$ , vs. field line latitude at 1100 km,  $\Lambda$ , for various magnetospheric configurations.  $B_d + B_s$  is the model described by Mead [1964].  $B_T(60\gamma)$  is an additional field component of magnitude  $60\gamma$ , solar oriented in the northern hemisphere and anti-solar oriented in the southern hemisphere.  $B_{CS}(40\gamma)$  is a current sheet in the magnetospheric tail yielding a  $40\gamma$  field adjacent to the sheet. See text for discussion.

5. Diagram showing coordinates used for computation of field due to truncated semi-infinite current sheet ( $B_{CS}$ ). This current sheet is coincident with the magnetic equatorial plane and extends radially from  $R_1$  to  $R_2$ . The sheet is infinite in length in a direction normal to the paper. The current flow is out of the paper.
6. Magnetospheric configuration obtained by addition of a current sheet in the magnetospheric tail of the model originally discussed by Mead [1964]. Dashed lines show field line configuration of the field due to the current sheet alone. Latitudes shown are latitudes at which field lines intersect the surface of the earth. This configuration was determined to give the best fit to experimental observations of trapped electron latitude shifts. See text for discussion.
7. Comparison of observed latitude shifts with predictions of various magnetospheric configurations. Data and calculations all on noon-midnight meridian. The  $\geq 280$  kev data points are taken from Figure 3 and are representative of high energy electrons in general. The curves are obtained directly from Figure 4 for the field configurations shown.
8. Comparison of the latitude shifts of  $\geq 40$  kev and  $\geq 280$  kev trapped electrons. The  $\geq 40$  kev data were obtained from the results of Frank et al [1964]. The figure shows the significantly larger shifts undergone by the lower energy trapped electron population.

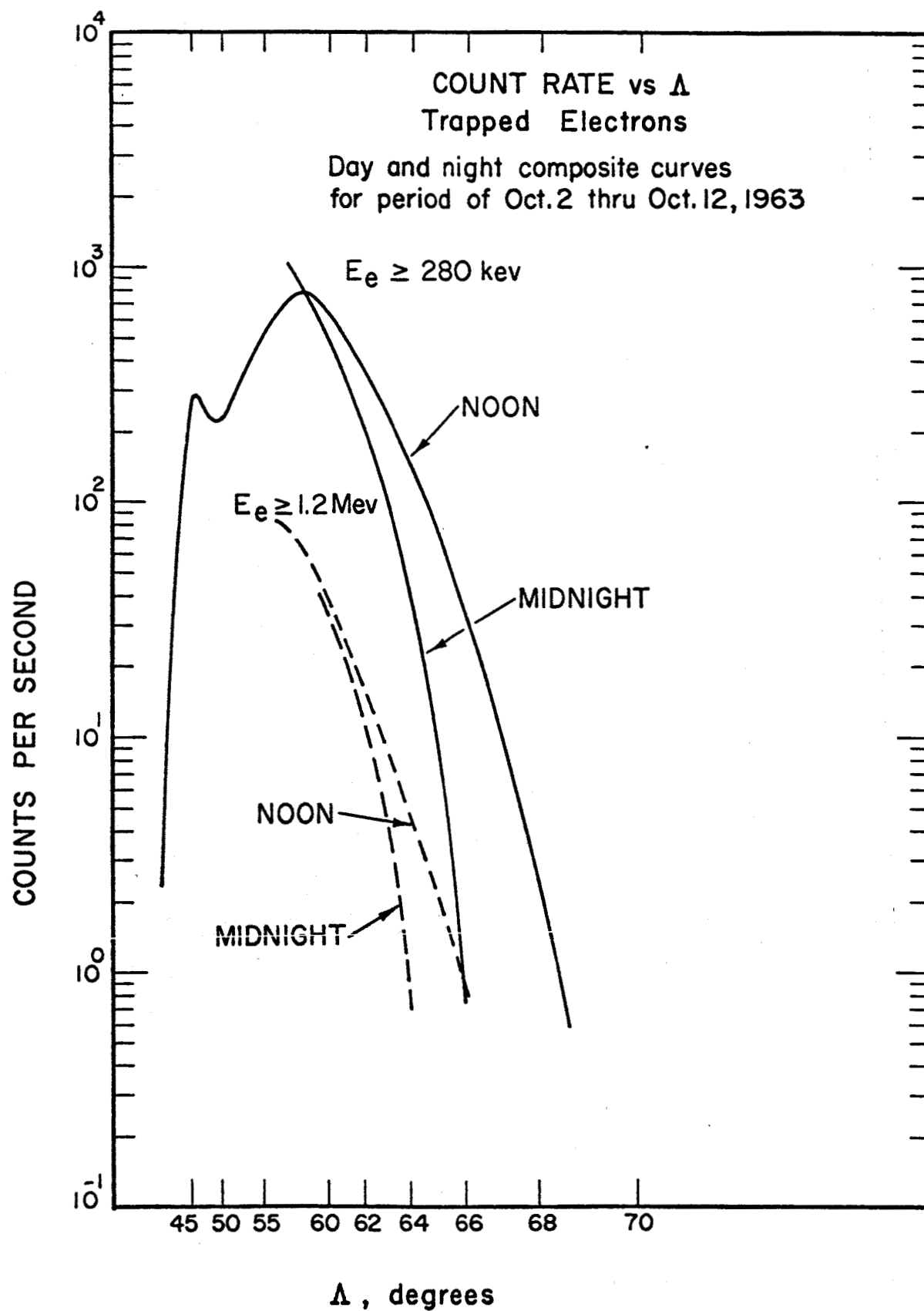


Fig. 1



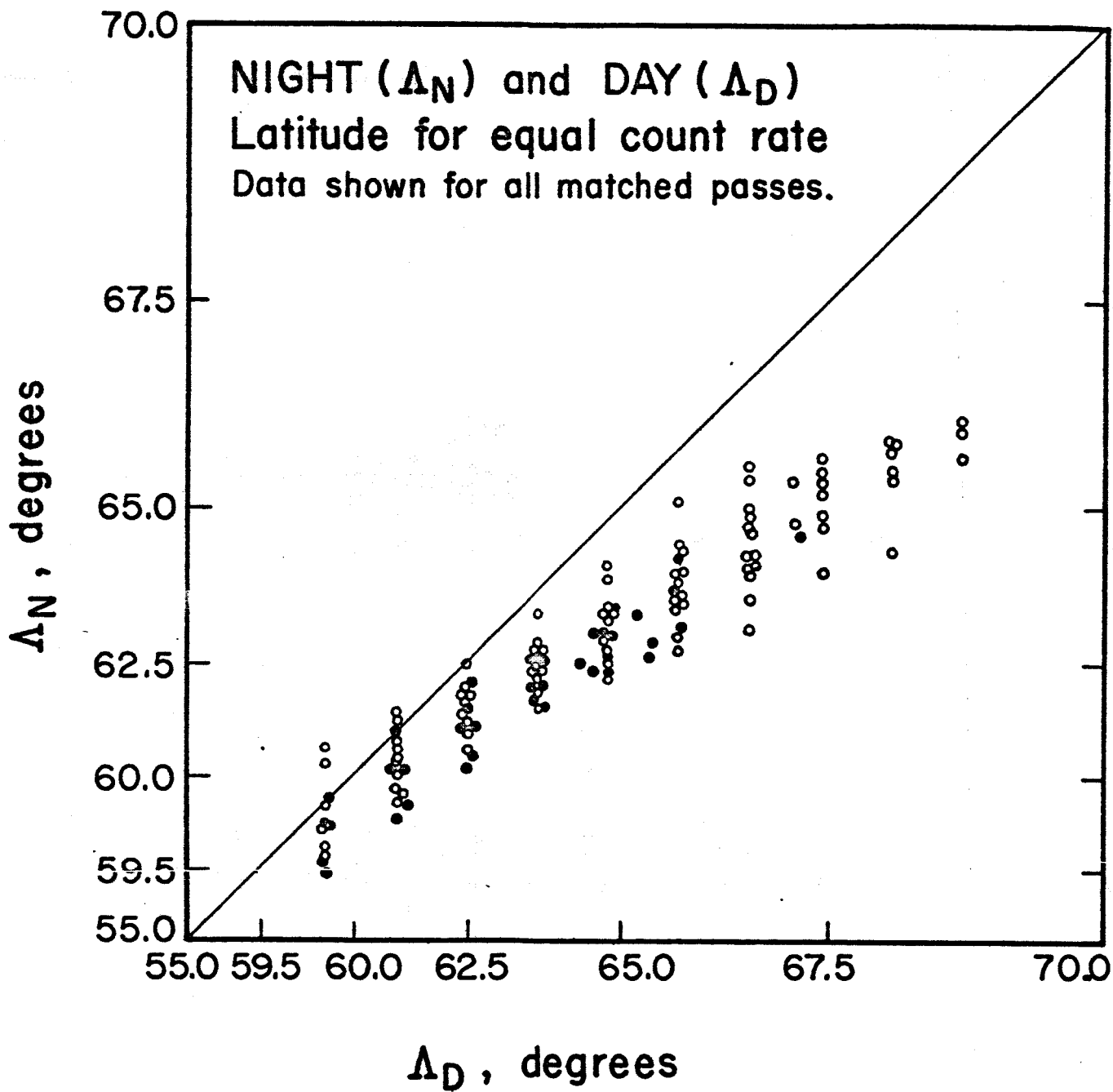


Fig. 2

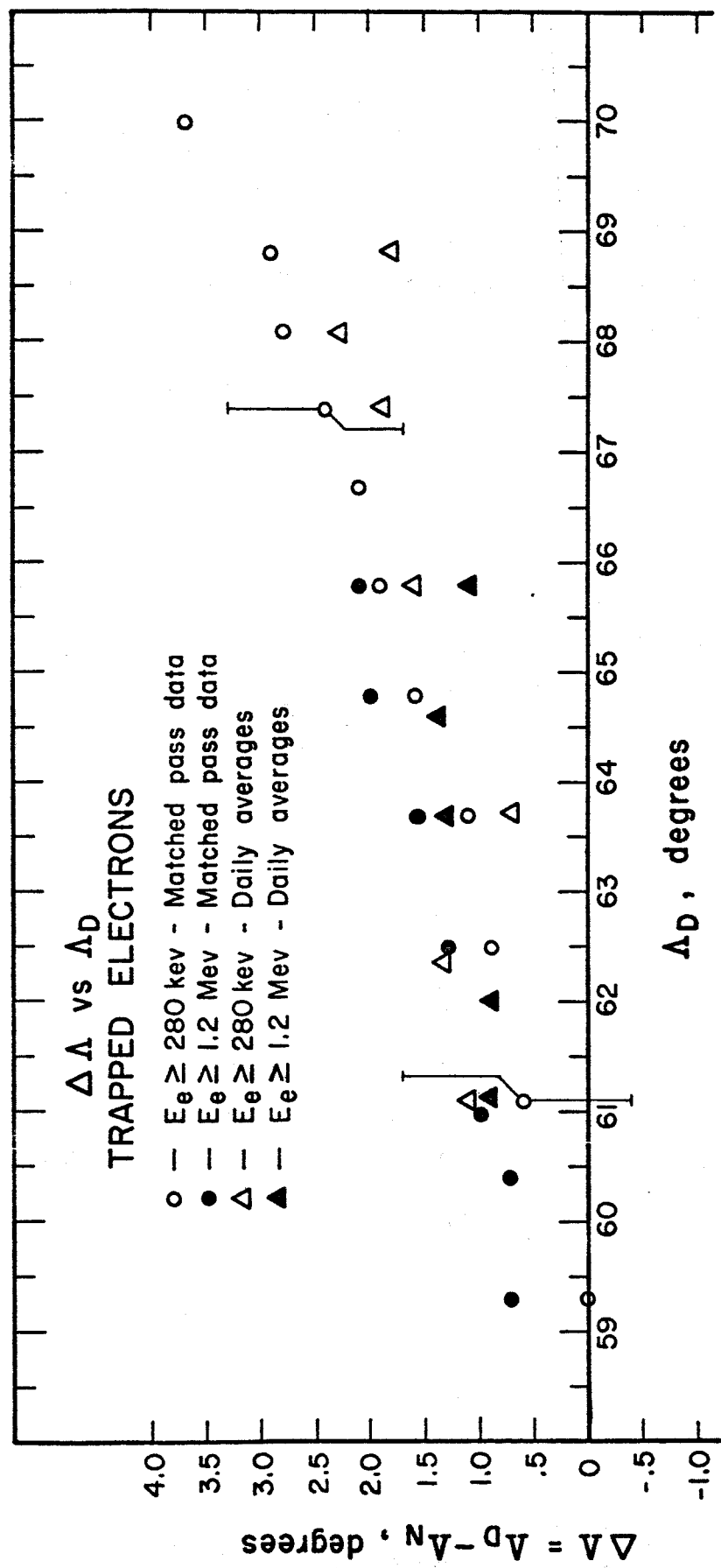


Fig. 3

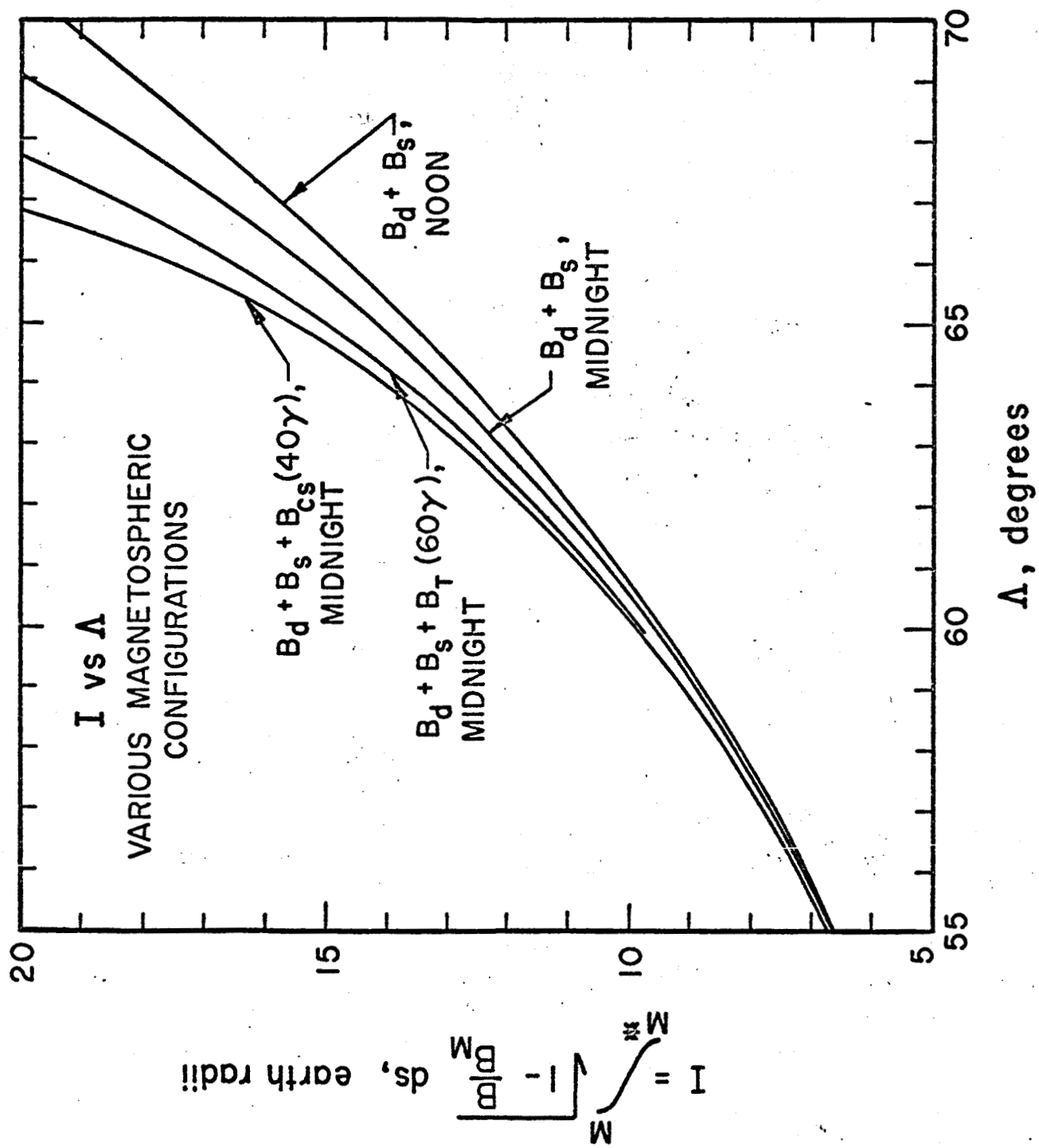


Fig. 4

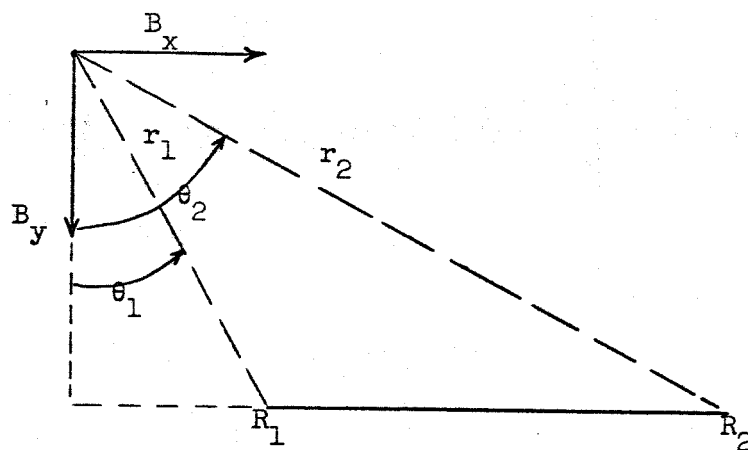


Figure 5

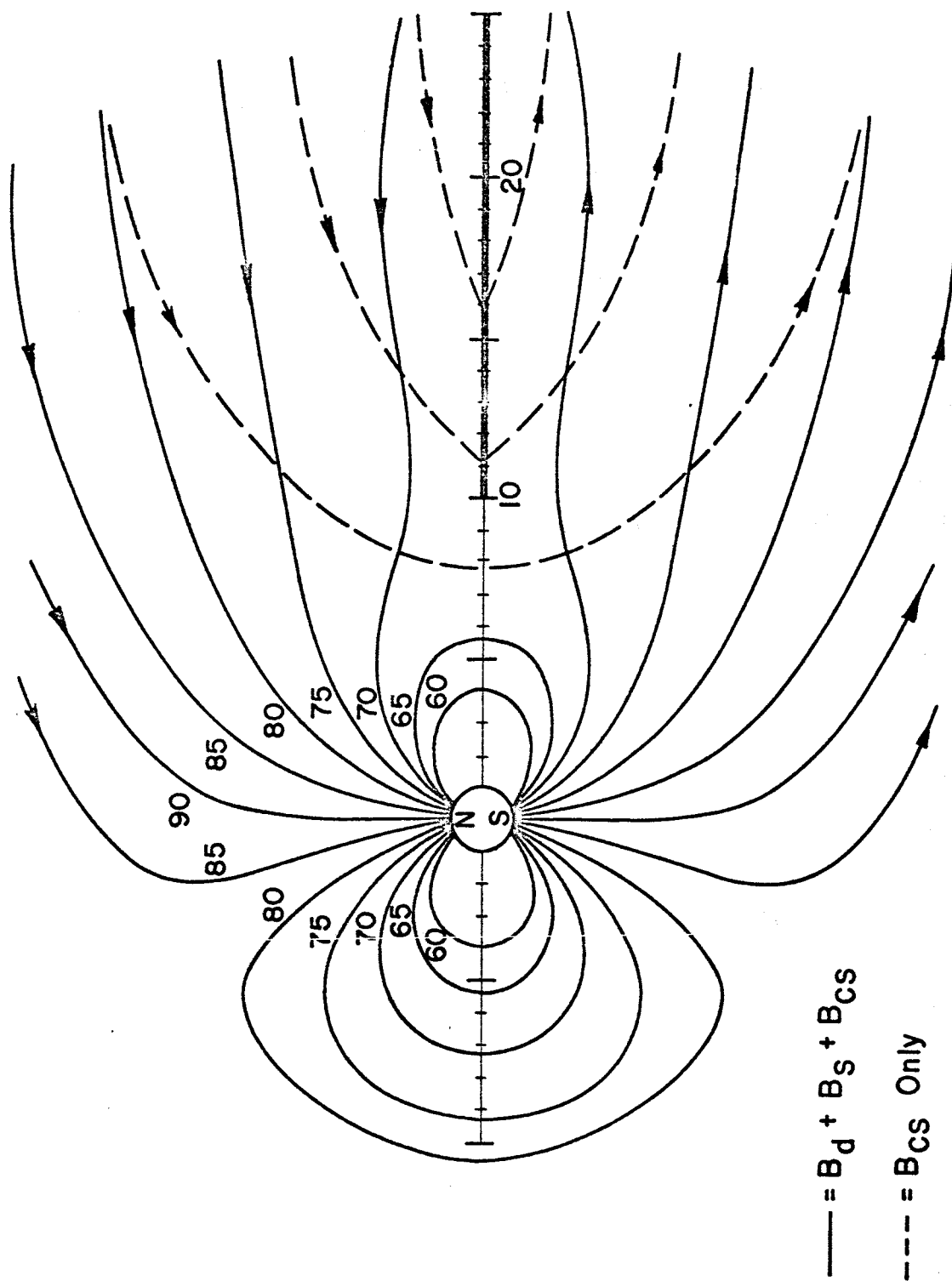


Fig. 6

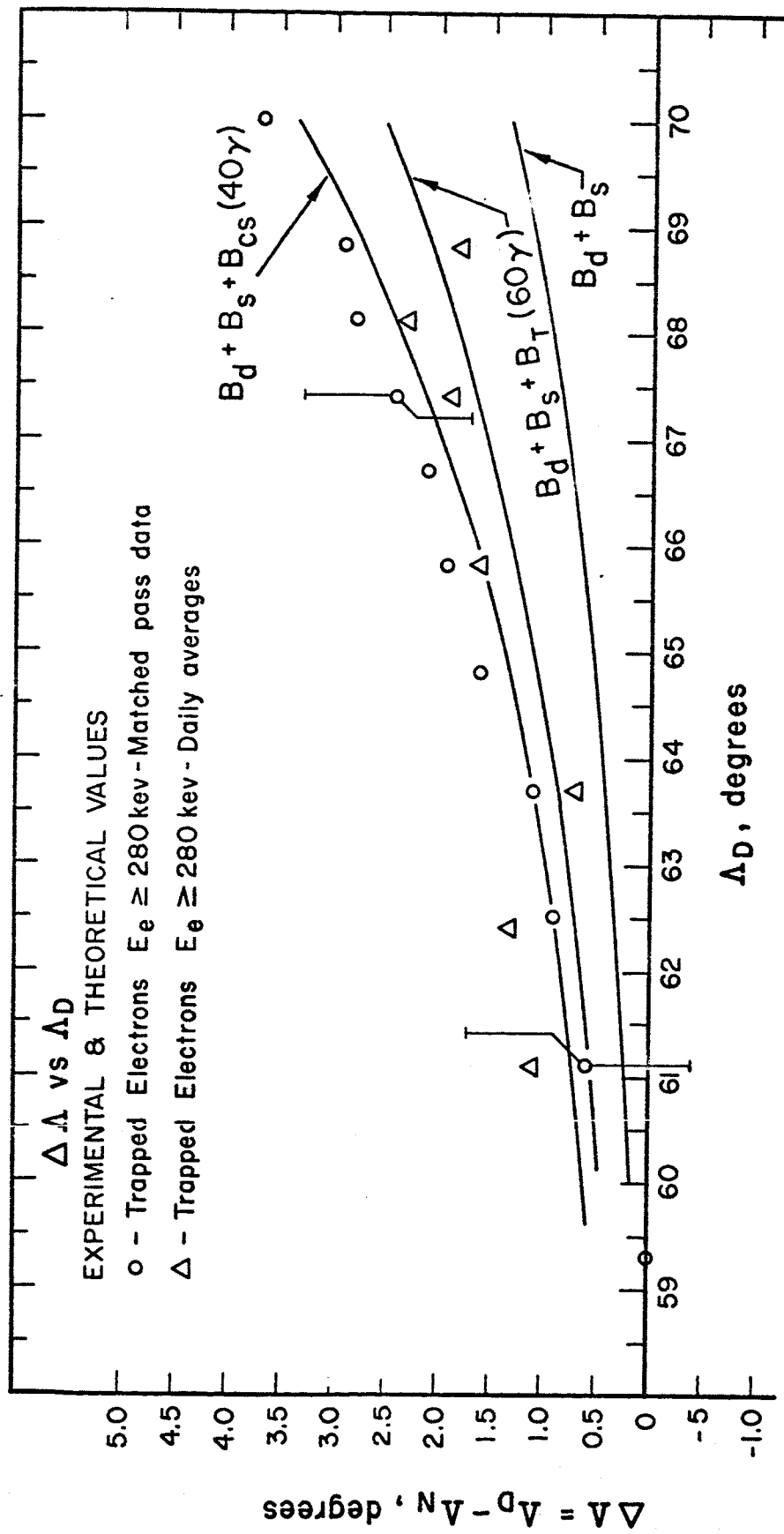


Fig. 7

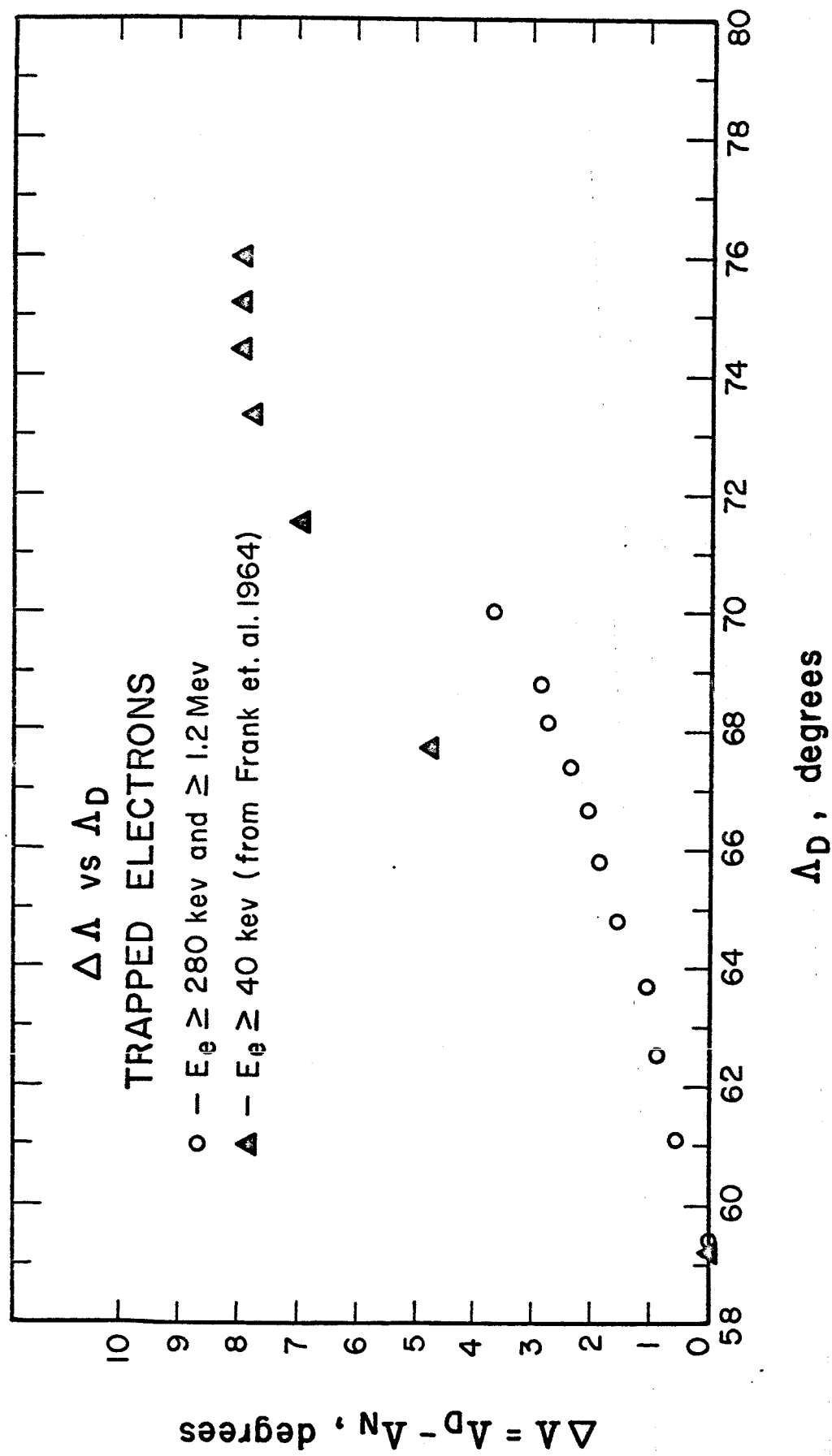


Fig. 8

## REFERENCES

- Axford, W. I., H. E. Petschek, and G. L. Siscoe, Tail of the magnetosphere, J. Geophys. Res., 70, 1231-1236, 1965.
- Dessler, A. J. and R. D. Juday, Configuration of auroral radiation in space, Planetary Space Sci., 13, 63-72, 1965.
- Fairfield, D. H., Trapped particles in a distorted dipole field, J. Geophys. Res., 69, 3919-3926, 1964.
- Frank, L. A., J. A. Van Allen, and J. D. Craven, Large diurnal variations of geomagnetically trapped and of precipitated electrons observed at low altitudes, J. Geophys. Res., 69, 3155-3168, 1964.
- Maeda, H., Electric fields in the magnetosphere associated with daily geomagnetic variations and their effects on trapped particles, J. Atmospheric Terrest. Phys., 26, 1133-1138, 1964.
- Malville, J. M., The effect of the initial phase of a magnetic storm upon the outer Van Allen belt, J. Geophys. Res., 65, 3008-3010, 1960.
- McDiarmid, I. B. and J. R. Burrows, High-latitude boundary of the outer radiation zone at 1000 km, Can J. Phys., 42, 616-626, 1964a.
- McDiarmid, I. B. and J. R. Burrows, Diurnal intensity variations in the outer radiation zone at 1000 km, Can J. Phys., 42, 1135-1148, 1964b.
- McIlwain, C. E., Coordinates for mapping the distribution of magnetically trapped particles, J. Geophys. Res., 66, 3681-3691, 1961.
- Mead, G. D., Deformation of the geomagnetic field by the solar wind, J. Geophys. Res., 69, 1169-1179, 1964.



Ness, N. F., The earth's magnetic tail, J. Geophys. Res., to be published, 1965. GSFC document X-612-64-392 (revised).

Ness, N. F., C. S. Scearce, and J. B. Seek, Initial results of the IMP 1 magnetic field experiment, J. Geophys. Res., 69, 3531-3569, 1964.

Northrop, T. G., Adiabatic charged particle motion, Rev. Geophys., 1, 283-304, 1963.

O'Brien, B. J., A large diurnal variation of the geomagnetically trapped radiation, J. Geophys. Res., 68, 989-998, 1963.

Williams, D. J. and J. W. Kohl, Loss and replenishment of electrons at middle latitudes and high B values, submitted to J. Geophys. Res., 1965.

Williams, D. J. and W. F. Palmer, Distortions in the radiation cavity as measured by an 1100 kilometer polar orbiting satellite, J. Geophys. Res., 70, 557-567, 1965.

Williams, D. J. and A. M. Smith, Daytime trapped electron intensities at high latitudes at 1100 kilometers, J. Geophys. Res., 70, 541-556, 1965.